医薬品または医療用具についての副作用，感染症および不具合報告の法制化に伴う実施要領の制定について」により，製造業者のみならず，医療機関からの報告事項について規定された。

感染因子について

感染とは，特に，病理学的には，生体内に侵入し，増殖の足がかりを確立すること，感染による発症は，宿主生体の諸種の抵抗力と微生物の状態や毒性などとの複雑な相互関係に依存する。感染因子には，ウイルス，リケッチア，クラミジア，マイコプラズマ，細菌，真菌，スピロヘータ，原虫，クロイツフェルト・ヤコブ病（CJD）などの感染病原体が含まれる。日本において，ヒト乾燥硬膜移植後の医原性CJDが明らかになり，また2001年9月には初のBSEが確認されたことから，プリオン病は大きな社会問題に発展している。プリオン病は，正常型プリオン蛋白質が異常感染型に構造変換することが原因となる神経変成疾患である。プリオン病は，ヒト，動物に見られる一群の神経変成疾患の呼称で，ヒトのクールー（kuru），Creuzfeldt–Jakob病（CJD），Gerstmann–Straussler–Scheinker病（GSS），致死性家族性不眠症（fatal familial insomnia；FFI），ヒツジのスクレイピー（scrapie），ウシ海綿状脳症（bovine spongiform encephalopathy：BSE）などが含まれる。感染型プリオン病では，プリオンが感染部位からリンパ臓器へ侵入してそこで増殖した後，自律神経繊維を介して中枢神経へ伝達されるという機序が最も中心的に働いていると推定されている。ウシ由来製品の医薬品などについては，製品の原料の切り換え，自主回収などのBSE対策措置が講じられ，BSEに対する理論的なリスクに対する予防的な安全対策がとられてきている。生物由来原料の安全性確保のためには，製造業者を含む関係者が責任をもって，常に新たな知見に基づく科学的水準でリスクを評価し，対応をとり続けていく必要性がある。（引用文献：ファルマシア 38，625–661，2002）。

今後

紙面の都合上，すべての改正内容について記載はできない。薬務関連の公報最新版

厚生労働省ホームページ：薬事法
http://www.hourei.mhlw.go.jp/~hourei/html/hourei/contents.html
審査管理課関連通知 http://www.nihs.go.jp/mhlw/tuuchi/index.html

を読み，正確な情報を入手することが重要である。

2003年10月25日医療機器フォーラム（http://dmd.nihs.go.jp/iryokiki/）設立記念シンポジウムを開催し，「Tissue Engineerin—開発と評価」に関する講演会を開いた。全国から多くの方々が参加された。医療機器フォーラムは，Tissue Engineering（細胞組織医療機器と名称されている。）を含む医療機器の健全な発展を図るために，医療機器の開発，製造および品質管理に係る問題について，産官学の情報交換の場を作ることを目的として設立した。

再生医療製品である細胞組織医療機器，医療材料，医療機器開発には，幅広い知識・経験・技術が必要である。多分野の専門家と協力し，これらの製品を必要とする患者さんに，安全で有効な製品を届けるために，開発に向かって，一丸となって進める時機にきている。

医療機器フォーラムは，毎年1回は定期的に開催（10〜11月頃予定）する予定である。安全かつ優れた医療機器（細胞組織医療機器，医療材料を含む）の開発支援に本フォーラムが有効に活用されることを願っている。

（医療機器フォーラムのホームページ：http://dmd.nihs.go.jp/iryokiki/）

（高分子学会発行「高分子」2004年3月号「細胞組織医療機器等の製品化のためのガイドライン，環境整備について」（執筆者同じ）に加筆して掲載）

（土屋　利江）

2　企業における再生医療への取り組みと動向

再生医療の現状を振り返るとき，その源流は，欧米，特にアメリカのベンチャー企業がもたらした，組織工学の商業化への取り組みに求めることができる。

1988年に開催されたアメリカの科学財団（NSF）による生体組織工学のワークショップにおいて，数社のベンチャー企業が製品化の努力をしていたことに関連して，産業化への予測がなされ，組織工学関連の世界における潜在的市場規模は年間約48兆円とも予測された[1]。また，VacantiとLangerの研究論文が認められたこと[2]により，組織工学が研究者，企業関係者の注目を浴びるようになり，その研究，開発が著しく進展した。

Gene expression changes in BALB/3T3 transformants induced by poly(L-lactic acid) or polyurethane films

Atsuko Matsuoka, Toshie Tsuchiya
Division of Medical Devices, National Institute of Health Sciences, 1-18-1 Kamiyoga, Setagaya-ku, Tokyo 158-8501, Japan

Received 26 March 2003; revised 9 July 2003; accepted 25 August 2003
Published online 19 December 2003 in Wiley InterScience (www.interscience.wiley.com). DOI: 10.1002/jbm.a.20068

Abstract: We performed DNA microarray analysis on two BALB/3T3 transformants (A5 and A6) induced by polyurethane (PU) film, two (L11 and L21) induced by biodegradable poly(L-lactic acid) (PLLA) film, and the parental cells. The transforming ability of the cells was in the order A5 < A6 < L21 < L11. In all, 1176 cancer-related genes were up- or down-regulated in at least one transformant. Those that were markedly up-regulated were c-*fos* protooncogene, FBJ osteosarcoma oncogene B, and Jun oncogene; those markedly down-regulated were pleiotrophin, histidine triad nucleotide-binding protein, protein kinase C iota, and large multifunctional protease 7. A common function of proteins encoded by genes that underwent marked expression changes was bone formation. The genes were c-*fos*, FBJ osteosarcoma, Jun, pleiotrophin, a disintegrin-like and metalloprotease with TS-1 motif protein 1. This finding was consistent with the tumor formation in the 2-year PLLA or PU subcutaneous implantation into rats. The number of genes that underwent marked expression change in each transformant was consistent with its malignancy. PLLA induced more malignant transformants than PU, especially in relation to osteosarcoma-like gene expression. © 2003 Wiley Periodicals, Inc. J Biomed Mater Res 68A: 376–382, 2004

Key words: BALB/3T3; transformation; PU; PLLA; DNA microarray analysis

INTRODUCTION

Polyurethanes (PUs) are widely used in medical devices because of their elasticity, high tensile strength, biocompatibility, and ease of handling. Poly(L-lactic acid) (PLLA) is used for bone screws and bone fixing plates because of its biodegradability. Some PUs, however, are unstable *in vivo* and induce tumors in rats.[1] Although there have been a number of *in vitro* studies on chemically induced transformation, few have analyzed the transformant DNA.

In the present study, we used DNA microarrays to analyze gene expression in transformants induced on high-molecular-weight polymer materials and related altered expression to the malignancy of the transformants, focusing on the consequences of transformation rather than on the process.

MATERIALS AND METHODS

Cells

Mouse Balb/3T3 clone A31-1-1 cells provided by Dr. T. Kuroki[2] (University of Tokyo) were maintained in minimum essential medium supplemented with 10% heat-inactivated fetal calf serum in 5% CO_2 in air at 37°C.

Correspondence to: A. Matsuoka; e-mail: matsuoka@nihs.go.jp

Materials

PU [MDI/PTMO 1000/BD, weight-averaged molecular weight (M_w) 220,000] was obtained from Sanyo-kasei Co. Ltd. and PLLA (M_w 200,000) films (thickness 0.3 mm) were obtained from Shimadzu Corporation.

Coating of materials on the glass dishes

PU was dissolved in tetrahydrofuran. Half the surface area of glass dishes (diameter 6 cm) was coated with 320 mg of PU. After the dishes dried, they were sterilized by autoclaving at 121°C for 15 min. In the case of PLLA, the film was cut to fit the bottom of plastic dishes (diameter 6 cm) and attached with a small amount of acetone. The acetone was evaporated completely and the dishes were sterilized under UV-irradiation for 2 h.

The transformation assay

Cells were seeded at a density of 1×10^4 /plate (diameter 6 cm) on a coating and cultured in medium that was changed twice per week. After 6 weeks, transformants were isolated and stored at −80°C.

TABLE I
Transformation Assay of PU- and PLLA-Induced Transformants and Parental Controls

Cell Line	Cloning Efficiency (% of Control)	No. of Foci/Plate[a]
A31-1-1	100	0.3 ± 0.48
A5	106.3	2.3 ± 1.23
A6	110.8	47.0 ± 6.28
L11	144.8	114.1 ± 13.32
L21	126.2	84.5 ± 5.10
A31-1-1 + MC[b]	2.2	30.0 ± 5.15

[a]Average with standard deviation of 15 plates.
[b]0.5 μg/mL (positive control).

Two transformants induced by PU (A5 and A6) and two induced by PLLA (L11 and L21) were thawed and cultured for confirmation of transformation and for DNA microarray analysis, which were conducted in parallel. For the positive control assay, cells were treated with 3-methylcholanthrene (MC, 0.5 μg/mL) 24 h after seeding, washed with fresh medium 72 h later, and incubated in normal medium up to 6 weeks. The number of transformed foci per plate served as malignancy of transformants.

DNA microarray analysis

At least 10^7 cells were harvested and frozen in liquid nitrogen. Total RNA was extracted, purified, assessed for yield and purity, and cDNA probes were synthesized with the Atlas™ Pure Total RNA Labeling System (Clontech) according to the manufacturer's instructions. Hybridization of the ^{33}P-labeled probes to the Atlas Array of Mouse Cancer 1.2 k Array (Clontec 7858-1), on which 1176 cDNAs of cancer-related genes were spotted, were performed with Atlas™ cDNA Expression Arrays according to the manufacturer's instructions. The phosphor images of hybridized arrays were analyzed with AtlasImage™ (Clontech). Genes that were up- or down-regulated more than fivefold relative to the negative controls are discussed.

RESULTS

The number of foci per dish produced by the selected transformants increased in the order A5 < A6 < L21 < L11 (Table I). The transformants isolated from PLLA were more malignant than those isolated from PU. A31-1-1 cells treated with MC induced 30 foci per plate, as expected. Figure 1 shows the actual foci features. The A5 and A6 foci resembled those on the MC-treated dishes. The extracellular matrix appeared lyzed in transformants L11 and L21.

Fourteen genes increased expression more than fivefold in at least one transformant (Fig. 2, Table II). The three most markedly up-regulated genes were c-*fos* protooncogene, FBJ osteosarcoma oncogene B, and Jun oncogene; all increased most in L11. The only

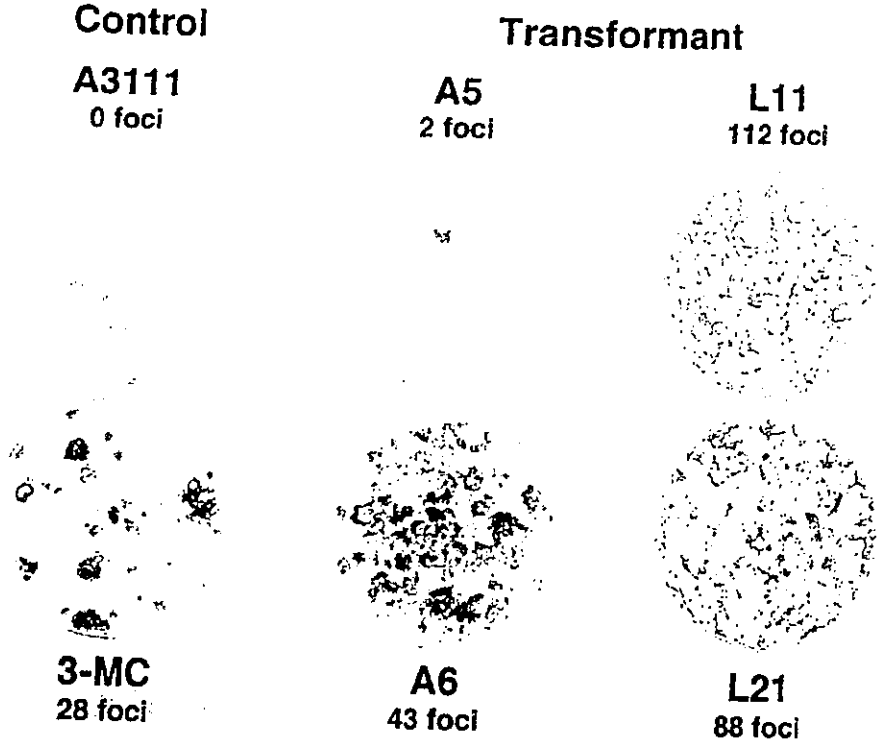

Figure 1. Photographs of dishes (6 cm in diameter) with Giemsa-stained foci in the confirmative transformation assay. The number of foci is shown in the representative plate of the control and each transformant. The control cells grew in monolayers and stained pink. The transformed cells stained blue were observed in the other plates, and the extracellular matrix of L11 and L21 plates appeared lyzed.

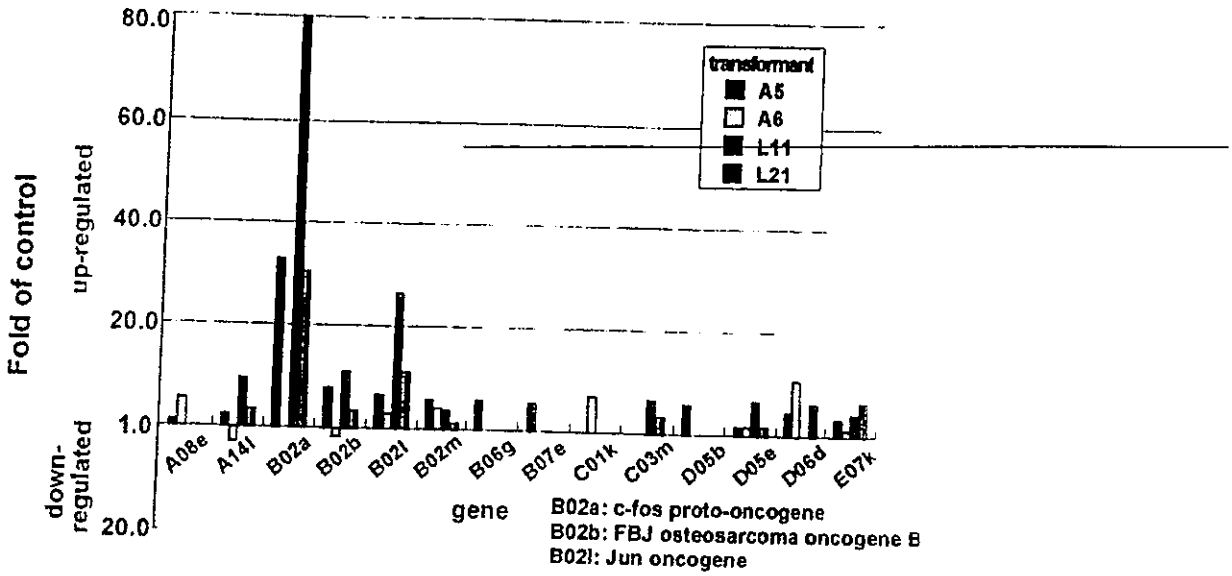

Figure 2. Expression profile of transformant genes whose expression increased more than fivefold in at least one transformant (see Table II for name key).

transformant that did not show any appreciable change in gene expression was A6.

Twenty-five genes decreased expression more than fivefold in at least one transformant (Fig. 3, Table III). The four most markedly down-regulated genes were pleiotrophin (PTN), histidine triad nucleotide-binding protein, protein kinase C iota, and large multifunctional protease 7; all except for large multifunctional protease 7, decreased most in L11. Transformant A6 showed a 20-fold decrease in the expression of large multifunctional protease 7.

Figure 4 shows the expression profiles of 30 oncogenes and tumor suppressor genes. *c-fos* Protooncogene, FBJ osteosarcoma oncogene B, and Jun oncogene were up-regulated markedly in transformants A5, L11, and L21 The expression levels of ras, src, raf, mitogen-activated protein kinases, MEK, and p53 were similar in parental cells and transformants within an approximate twofold increase or decrease

Among the extracellular matrix-related genes, HSP60, HSP65, HSPD1, mitochondrial matrix protein P1 precursor, 60-kDa chaperonin, GroEL protein, and matrix metalloproteinase 9 were markedly down-regulated, especially in transformant L11 (Fig. 5).

Expression of transforming growth factor (TGF) β1 and 2 and 8 connexin-related genes did not change significantly in any transformants (data not shown).

Table IV lists the genes that were up- or down-regulated more than fivefold relative to parental controls. Large multifunctional protease 7 was down-regulated more than fivefold, in all transformants. The gene expression profile of A6 was unique among the

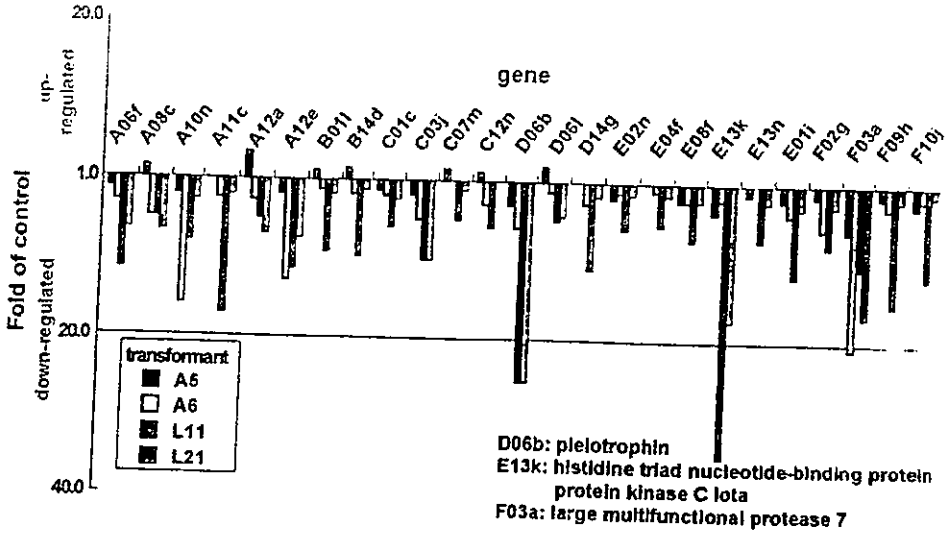

Figure 3. Expression profile of transformant genes whose expression decreased more than fivefold in at least one transformant (see Table III for name key).

TABLE II
Transformant Genes Whose Expression Increased More Than Fivefold

Code	Gene
A08e	Integrin β 7
A14l	Insulin-like growth factor binding protein 10
B02a	*c-fos* protooncogene
B02b	FBJ osteosarcoma oncogene B
B02l	Jun oncogene
B02m	*junB* protooncogene
B06g	HSP27, HSP25, HSPB1, growth-related 25-kDa protein
B07e	N-oxide forming dimethylaniline monooxygenase 1, hepatic flavin-containing monooxygenase 1, dimethylaniline oxidase 1
C01k	Retinoic acid receptor β, nuclear receptor subfamily 1 group B member 2
C03m	Caspase-activated DNase, DNase inhibited by DNA fragmentation factor
D05b	Insulin-like growth factor II precursor, multiplication-stimulating polypeptide
D05e	Leukemia inhibitory factor, cholinergic differentiation factor
D06d	Proliferin
E07k	Nonreceptor type 16 protein tyrosine phosphatase

four transformants in that proliferin was up-regulated more than 10-fold, thrombospondin 1 (TS-1) was down-regulated more than 10-fold, and large multifunctional protease 7 was down-regulated more than 20-fold. L11 showed the most appreciable changes in expression intensity and in the number of genes down-regulated. In that transformant, *c-fos* protooncogene and Jun oncogene were markedly up-regulated whereas PTN, histidine triad nucleotide-binding protein, and protein kinase C iota were markedly down-regulated. L21 showed marked up-regulation in the expression of *c-fos* protooncogene and Jun oncogene and marked down-regulation in the expression of PTN, histidine triad nucleotide-binding protein, protein kinase C iota, and large multifunctional protease 7.

The only significant association we observed between changes in gene expression and malignancy were for cellular tumor antigen p53, procollagen VI alpha 3 subunit, and connexin 43. The relationship was inverse and was observed when the decrease in expression was less than fivefold (data not shown).

DISCUSSION

DNA microarray analysis of two transformants (A5 and A6) induced on PU film and two (L11 and L21) induced on PLLA film showed L11 to be the most malignant and the one that underwent the most appreciable changes in gene expression levels.

Both *c-fos* and Jun were up-regulated in all transformants except A6. *c-fos*, a protooncogene, is the cellular homolog of *v-fos*, which was originally isolated from a murine osteosarcoma. Fos protein is a major component of the AP-1 transcription factor complex, which includes the jun family. In the present study, the genes involved in bone formation, namely *c-fos*, FBJ osteosarcoma oncogene B, Jun, PTN, ADAM-TS, and MMP9, were among those that changed expression levels (Table IV). They were up- or down-regulated markedly in L21 and even more so in L11. Wang et al.[3] demonstrated in transgenic and chimeric mice that overexpression of *c-fos* affects bone, cartilage, and hematopoietic cell development. Wang et al.[4] also showed that mice lacking *c-fos* are growth retarded, develop osteopetrosis with deficiencies in bone remodeling and tooth eruption, and have altered hematopoiesis. Onyia et al.,[5] investigating gene expression in rat osteoblast-like osteosarcoma cells (ROS 17/2.8) cultured *in vivo*, demonstrated that at 56 days, *c-fos* expression increased up to fivefold, *c-jun* expression increased 2.1-fold, and MMP-9 expression decreased to undetectable levels. Those findings are consistent with the present finding in L11, that is, that *jun*, *fos*,

TABLE III
Transformant Genes Whose Expression Decreased More Than Fivefold

Code	Gene
A06f	Cdk 6 inhibitor, Cdk 4 inhibitor C, Cdk inhibitor 2C
A08c	Fat tumor suppressor homolog (*Drosophila*)
A10n	Thrombospondin 1
A11c	VCAM-1 precursor
A12a	Cysteine-rich intestinal protein
A12e	Delta-like homolog 1, preadipocyte factor 1, SCP 1, FA1, ZOG
B01l	EB1 APC-binding protein
B14d	HSP60, HSP65, HSPD1, mitochondrial matrix protein P1 precursor, 60-kDa chaperonin, GroEL protein
C01c	Apoptosis inhibitor 1
C03j	Clusterin precursor, clustrin, apolipoprotein J, sulfated glycoprotein 2
C07m	Platelet-derived growth factor receptor α precursor
C12n	Hek2 murine homolog, Mdk5 mouse developmental kinase, Eph-related tyrosine-protein kinase receptor
D06b	PTN
D06l	Small inducible cytokine A9
D14g	Avian sarcoma virus CT10 (*v-crk*) oncogene homolog
E02n	Nonreceptor type 11 protein tyrosine phosphatase, phosphotyrosine phosphatase
E04f	Cdk7, CDC2-related kinase 4, Cdk-activating kinase, 39-kDa protein kinase, MO15, MPK7
E08f	Serum-inducible kinase
E13k	Histidine triad nucelotide-binding protein, protein kinase C iota
E13n	Menage a trois 1
F01i	A disintegrin-like and metalloprotease with thrombospondin type 1 motif protein 1
F02g	Matrix metalloproteinase 9
F03a	Large multifunctional protease 7
F09h	Developmentally d neural precursor cell expressed
F10j	Tubulin cofactor a

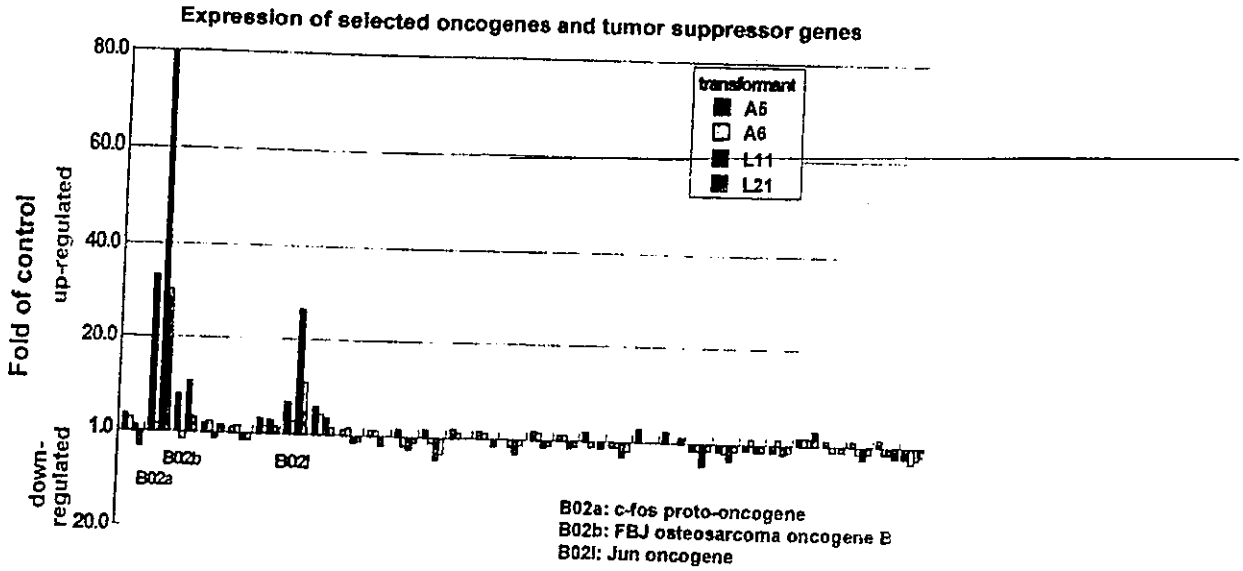

Figure 4. Expression profile of transformant oncogenes and tumor suppressor genes. Thirty-nine spots of oncogene- and tumor suppressor gene-related genes were on the DNA tip and 30 of them were analyzable, but not in all transformants. Only those genes whose expression level changed at least fivefold are named.

and osteosarcoma genes were up-regulated whereas MMP9 was down-regulated, suggesting that PLLA stimulated BALB/3T3 cells to express genes related to osteogenesis.

Nakamura et al.[6] observed bone formation in 6 of 22 tumors induced in rats by a 2-year PLLA subcutaneous implantation. Tumor incidence was 44% (22/50) with PLLA[6] and 38% (11/29) with PU,[1] which correlates well with the *in vitro* malignancy incidence data in the present study. Isama and Tsuchiya,[7] and Ikarashi et al.[8] reported that low-molecular-weight PLLA increases alkaline phosphatase activity and stimulates calcification of mouse osteoblast-like MC3T3-E1 cells.

PTN, a heparin-binding protein that can function as a neurite-promoting factor[9] or a mitogenic factor for fibroblasts,[10] contains two β-sheet domains that correspond to TS-1 repeats.[11] The expression of PTN is increased in various human tumors, suggesting it as a tumor marker and a target for tumor therapy. PTN was shown to regulate bone morphogenetic protein-induced ectopic osteogenesis in rats.[12]

A disintegrin-like and metalloprotease with TS-1 motif protein 1 (ADAM-TS) is a family of zinc-dependent proteases that has an important role in a variety of normal and pathological conditions such as arthritis and cancer. They consist of a signal sequence, a propeptide, a metalloproteinase domain, a disintegrin-like domain, a cysteine-rich region, and a variable number of TS-1 repeats. High levels of their tran-

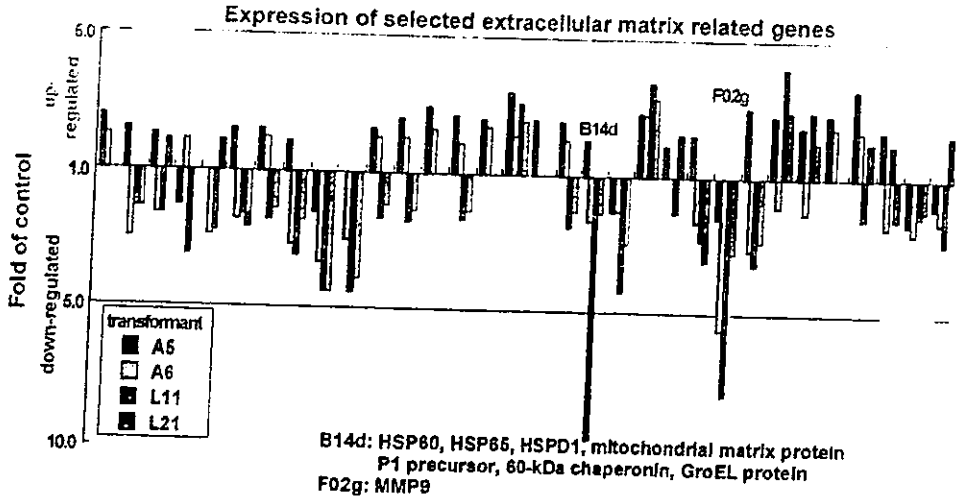

Figure 5. Gene expression profile of extracellular matrix-related genes. Thirty-two extracellular matrix-related genes were analyzable but data were not available in some transformants even in them. The code and name of genes whose expression changed fivefold or less are not shown. L11 showed clear down-regulation in expression of genes of codes B14d and F02g.

TABLE IV
Transformant Genes Whose Expression Increased or Decreased More Than Fivefold of Controls[a]

Transformant	Up-Regulated	Down-Regulated
A5	**c-*fos* protooncogene (33.0)**	Large multifunctional protease 7
	FBJ osteosarcoma oncogene B	
	Jun oncogene	
	*jun*B protooncogene	
	HSP27, HSP25, HSPB1, growth-related 25-kDa protein	
	N-oxide forming dimethylaniline monooxygenase 1, hepatic flavin-containing monooxygenase 1, dimethylaniline oxidase 1	
	Insulin-like growth factor II precursor, multiplication-stimulating polypeptide	
A6	Integrin β 7	Fat tumor suppressor homolog (*Drosophila*)
	Retinoic acid receptor β, nuclear receptor subfamily 1 group B member 2	**Thrombospondin 1 (15.8)**
	Proliferin (10.7)	**Delta-like homolog 1, preadipocyte factor 1, SCP 1, FA1, ZOG (12.7)**
		Clusterin precursor, clustrin, apolipoprotein J, sulfated glycoprotein 2
		PTN
		Matrix metalloproteinase 9
		Large multifunctional protease 7 (20.7)
L11	Insulin-like growth factor binding protein 10	**Cdk 6 inhibitor, Cdk 4 inhibitor C, Cdk inhibitor 2C (11.5)**
	c-*fos* protooncogene (79.8)	Fat tumor suppressor homolog (*Drosophila*)
	FBJ osteosarcoma oncogene B (10.9)	Thrombospondin 1
	Jun oncogene (26.3)	**VCAM-1 precursor (17.0)**
	Caspase-activated DNase, DNase inhibited by DNA fragmentation factor	**Delta-like homolog 1, preadipocyte factor 1, SCP 1, FA1, ZOG (11.2)**
	Leukemia inhibitory factor, cholinergic differentiation factor	EB1 APC-binding protein
		HSP60, HSP65, HSPD1, mitochondrial matrix protein P precursor, 60-kDa chaperonin, GroEL protein
		Apoptosis inhibitor 1
		Clusterin precursor, clustrin, apolipoprotein J, sulfated glycoprotein 2 (10.0)
		Platelet-derived growth factor receptor α precursor
		Hek2 murine homolog, Mdk5 mouse developmental kinase, Eph-related tyrosine-protein kinase receptor
		PTN (25.2)
		Small inducible cytokine A9
		Avian sarcoma virus CT10 (v-*crk*) oncogene homolog (11.0)
		Nonreceptor type 11 protein tyrosine phosphatase, phosphotyrosine phosphatase
		Cdk7, CDC2-related kinase 4, Cdk-activating kinase, 39-kDa protein kinase, MO15, MPK7
		Serum-inducible kinase
		Histidine triad nucelotide-binding protein, protein kinase C iota (34.4)
		Menage a trois 1
		A disintegrin-like and metalloprotease with thrombospondin type 1 motif protein 1 (11.8)
		Matrix metalloproteinase 9
		Large multifunctional protease 7 (10.4)
		Developmentally d neural precursor cell expressed (15.0)
		Tubulin cofactor a (11.8)
L21	c-*fos* protooncogene (30.3)	Cdk 6 inhibitor, Cdk 4 inhibitor C, Cdk inhibitor 2C
	Jun oncogene (11.1)	Fat tumor suppressor homolog (*Drosophila*)
	Proliferin	Cysteine-rich intestinal protein
	Nonreceptor type 16 protein tyrosine phosphatase	Delta-like homolog 1, preadipocyte factor 1, SCP 1, FA1, ZOG
		Clusterin precursor, clustrin, apolipoprotein J, sulfated glycoprotein 2 (10.0)
		PTN (25.2)
		Histidine triad nucleotide-binding protein, protein kinase C iota (17.2)
		Large multifunctional protease 7 (16.6)

[a]Genes in regular and bold text were up- or down-regulated between 5- and 10-fold, and more than 10-fold, respectively. Figures in parentheses indicate fold-increase or -decrease in gene expression compared with parental cells.

scripts are observed in some tumor biopsies and cell lines, including osteosarcomas, melanoma, and colon carcinoma cells.[13,14]

Vascular cell adhesion molecule 1 (VCAM-1) is inducible by inflammatory cytokines and lipopolysaccharides such as interleukin 1, tumor necrosis factor α, interferon γ, and interleukin 4. It functions by binding with integrin $\alpha_4\beta_1$. Kawaguchi and Ueda[15] reported that VCAM-1 was not expressed in the seven osteosarcoma specimens tested in a study on the distribution of integrins and their matrix ligands in osteogenic sarcomas. Those results agree with the finding in the present study that osteosarcoma-like gene expression was down-regulated in L11.

BALB/3T3 cells are sensitive to transformation and must be handled carefully. Repeated subculture and overgrowth are not advised. We cultured the isolated foci under constant conditions to investigate the difference in gene expression. Because DNA microarray analysis was done only once, we discussed only genes that showed clear differences in expression from the controls. Based on these preliminary data, further studies are needed to confirm bone formation by PU and PLLA.

CONCLUSIONS

The gene that showed the greatest change in expression after cell culture on PU was c-*fos* protooncogene. Osteogenesis was a common function of proteins encoded by genes that underwent a marked change in expression. Although the changes in gene expression induced by PU and PLLA differed in intensity, the results were consistent with previously reported findings of *in vivo* tumor formation. PLLA had a greater effect than PU on the expression levels of genes related to bone formation. In the transformants, both up-regulation of oncogenes and down-regulation of other kinds of genes were induced, and the latter appeared to be more related to the malignancy of transformants than the former.

References

1. Nakamura A, Kawasaki Y, Takeda K, Aida Y, Kurokawa Y, Kojima S, Shintani H, Matsui M, Nohmi T, Matsuoka A, Sofuni T, Kurihara M, Miyata N, Uchida T, Fujimaki M. Difference in tumor incidence and other tissue responses to polyetherurethanes and polydimethylsiloxane in long-term subcutaneous implantation into rats. J Biomed Mater Res 1992;26:631–650
2. Kuroki T, Drevon C. Inhibition of chemical transformation in C3H/10T1/2 cells by protease inhibitors. Cancer Res 1979;39: 2755–2761.
3. Wang ZQ, Grigoriadis AE, Mohle-Steinlein U, Wagner EF. A novel target cell for c-*fos*-induced oncogenesis: development of chondrogenic tumors in embryonic stem cell chimeras. EMBO J 1991;10:2437–2450.
4. Wang ZQ, Ovitt C, Grigoriadis AE, Mohle-Steinlein U, Ruther U, Wagner EF. Bone and haematopoietic defects in mice lacking c-*fos*. Nature 1992;360:741–745.
5. Onyia JE, Hale LV, Miles RR, Cain RL, Tu Y, Hulman JF, Hock JM, Santerre RF. Molecular characterization of gene expression changes in ROS 17/2.8 cells cultured in diffusion chambers *in vivo*. Calcif Tissue Int 1999;65:133–138.
6. Nakamura T, Shimizu Y, Okumura N, Matsui T, Hyon S-H, Shimamoto T. Tumorigenicity of poly-L-lactide (PLLA) plates compared with medical-grade polyethylene. J Biomed Mater Res 1994;28:17–25.
7. Isama K, Tsuchiya T. Effect of γ-ray irradiated poly(L-lactide) on the differentiation of mouse osteoblast-like MC3T3-E1 cells. J Biomater Sci Polym Ed 2002;13:153–166
8. Ikarashi Y, Tsuchiya T, Nakamura A. Effect of heat treatment of poly(L-lactide) on the response of osteoblast-like MC3T3-E1 cells. Biomaterials 2000;21:1259–1267.
9. Rauvala H. An 18-kd heparin-binding protein of developing brain that is distinct from fibroblast growth factors. EMBO J 1989;8:2933–2941.
10. Milner PG, Li YS, Hoffman RM, Kodner CM, Siegel NR, Deuel TF. A novel 17 kD heparin-binding growth factor (HBGF-8) in bovine uterus: purification and N-terminal amino acid sequence. Biochem Biophys Res Commun 1989;165:1096–1103
11. Klipelainen I, Kaksonen M, Avikainen H, Fath M, Linhardt RJ, Raulo E, Rauvala H. Heaprin-binding growth-associated molecule contains two heparin-binding beta-sheet domains that are homologous to the thrombospondin type I repeat. J Biol Chem 2000;275:13564–13570.
12. Sato Y, Takita H, Ohata N, Tamura M, Kuboki Y. Pleiotrophin regulates bone morphogenetic protein (BMP)-induced ectopic osteogenesis. J Biochem 2002;131:877–886.
13. Cal S, Arguelles JM, Fernandez PL, Lopez-Otin C. Identification, characterization, and intracellular processing of ADAM-TS12, a novel human disintegrin with a complex structural organization involving multiple thrombospondin-1 repeats. J Biol Chem 2001;276:17932–17940.
14. Cal S, Obaya AJ, Llamazares M, Garabaya C, Quesada V, Lopez-Otin C. Cloning, expression analysis, and structural characterization of seven novel human ADAMTSs, a family of metalloproteinases with disintegrin and thrombospondin-1 domains. Gene 2002;283:49–62.
15. Kawaguchi S, Ueda T. Distribution of integrins and their matrix ligands in osteogenic sarcomas. J Orthop Res 1993;11:386–395.

ACADEMIC PRESS

Available online at www.sciencedirect.com

SCIENCE DIRECT®

Analytical Biochemistry 316 (2003) 15–22

ANALYTICAL BIOCHEMISTRY

www.elsevier.com/locate/yabio

Microanalysis of N-linked oligosaccharides in a glycoprotein by capillary liquid chromatography/mass spectrometry and liquid chromatography/tandem mass spectrometry

Nana Kawasaki,* Satsuki Itoh, Miyako Ohta, and Takao Hayakawa

Division of Biological Chemistry and Biologicals, National Institute of Health Sciences, 1-18-1, Kamiyoga, Setagaya-ku, Tokyo 158-8501, Japan

Received 5 August 2002

Abstract

We have studied rapid and simple sugar mapping using liquid chromatography/electrospray ionization mass spectrometry (LC/MS) equipped with a graphitized carbon column. The oligosaccharide mixture was separated on the basis of the sequence, branching structure, and linkage, and each oligosaccharide was characterized based on its molecular mass. In this study we demonstrated the usefulness of capillary LC/MS (CapLC/MS) and capillary liquid chromatography/tandem mass spectrometry (CapLC/MS/MS) as sensitive means for accomplishing the structural analysis of oligosaccharides in a low-abundance glycoprotein. The carbohydrate heterogeneity and molecular mass information of each oligosaccharide can be readily obtained from CapLC/MS of a small amount of glycoprotein. CapLC/MS/MS provided b-ion series, which is informative with regard to monosaccharide sequence. Exoglycosidase digestion followed by CapLC/MS elucidated a carbohydrate residue linkage. Using this method, we characterized N-linked oligosaccharides in hepatocyte growth factor produced in mouse myeloma NS0 cells as the complex-type bi-, tri-, and tetraantennary terminated with *N*-glycolylneuraminic acids and α-linked galactose residues. Sugar mapping with CapLC/MS and CapLC/MS/MS is useful for monitoring glycosylation patterns and for structural analysis of carbohydrates in a low-abundance glycoprotein and thus will become a powerful tool in biological, pharmaceutical, and clinical studies.

Keywords: Capillary LC/MS; Capillary LC/MS/MS; Glycoprotein; Oligosaccharide; Hepatocyte growth factor

A large number of cellular proteins have been analyzed in recent years in an attempt to understand their structures, functions, and networks. It has been suggested that most common proteins are glycosylated and exist in different forms due to the heterogeneity of glycosylation. Glycosylation is known to play an important role in biological function, dynamics, and physicochemical properties such as folding, solubility, aggregation, and stability [1]. There are many examples in which alteration in glycosylation may be linked to diseases [2]. The characterization of glycosylation in proteins is clearly important.

Sugar mapping using HPLC has proven to be useful for extensive separation of diverse oligosaccharide mixtures [3–5]. Oligosaccharides released from a glycoprotein are visualized by derivation and are characterized based on their elution times. We previously reported that mass spectrometric sugar mapping using liquid chromatography/electrospray ionization mass spectrometry (LC/MS)[1] equipped with a graphitized carbon column (GCC) can be a powerful tool for the structural analysis of oligosaccharides [6–9]. Oligosaccharides in mixture can be separated, and each oligosaccharide can be characterized based on its retention

* Corresponding author. Fax: +81-3-3707-6950.
E-mail address: nana@nihs.go.jp (N. Kawasaki).

[1] *Abbreviations used:* Ac, acetyl; Bi, biantennary; Cap, capillary; CID, collision induced dissociation; EPO, erythropoietin; ESI, electrospray ionization; GCC, graphitized carbon column; GlcNAc, *N*-acetylglucosamine; Hex, hexose; HGF, hepatocyte growth factor; Fuc, fucose; Lac, *N*-acetyllactosamine; LC/MS, liquid chromatography/mass spectrometry; LC/MS/MS, liquid chromatography/tandem mass spectrometry; NeuAc, *N*-acetylneuraminic acid; NeuGc, *N*-glycolylneuraminic acid; PNGase F, *N*-glycosidase F; Tetra, tetraantennary; Tri, triantennary.

0003-2697/03/$ - see front matter © 2003 Elsevier Science (USA). All rights reserved.
doi:10.1016/S0003-2697(03)00031-9

time and molecular mass without it being a time-consuming process. The utility of this method has recently been demonstrated by the simultaneous analysis of high-mannose-type, hybrid-type, and sialylated and nonsialylated complex-type N-linked oligosaccharides [10]. The usefulness of LC/MS for the structural analysis of O-linked oligosaccharides and derived oligosaccharides has also been reported by other groups [11–14].

Two-dimensional polyacrylamide gel electrophoresis is the most widely used method for the separation of complex cellular protein mixtures. Protein identification is achieved by MS of proteolytic peptides extracted from the gel. Carbohydrate structures are deduced from the mass spectra of the glycopeptides; however, carbohydrate heterogeneity and structural details, including monosaccharide sequence, branching structure, and linkages, cannot be elucidated by the MS of glycopeptides. Sugar mapping of gel-separated glycoproteins is useful for analyzing the structure and function of glycosylation. The amount of proteins separated by electrophoresis has been in the range 1 to 50 μg, which requires a sensitive means for the sugar mapping. Here we have extended the mass spectrometric sugar mapping for a small amount of glycoprotein by using a capillary LC/MS with a nanoelectrospray ion source (CapLC/MS) and CapLC/MS/MS. We have also demonstrated the application of the method to the structural analysis of N-linked oligosaccharides from hepatocyte growth factor (HGF).

Materials and methods

Materials

Recombinant human HGF expressed in a mouse myeloma cell line, NS0, was purchased from Genzyme (Cambridge, MA, USA). *N*-Glycosidase F (PNGase F) and α-galactosidase (green coffee beans) were obtained from Roche Diagnostics GmbH (Mannheim, Germany) and Glyko, Inc. (Novato, CA, USA), respectively. All other chemicals used were of the highest purity available.

Preparation of borohydrade-reduced oligosaccharides

HGF (25 μg) was dissolved in 50 μl of phosphate-buffered saline and incubated with 1% Triton X-100 and 4 units of PNGase F at 37 °C for 6 days. Protein was precipitated with 224 μl of cold ethanol. The supernatant was dried, and the oligosaccharides were dissolved in 50 μl of H_2O. To the oligosaccharide solution was added 0.5 M $NaBH_4$ (50 μl), and the mixture was incubated at 25 °C for 2 h. Diluted acetic acid (10 μl) was added to the mixture to decompose excess $NaBH_4$. The reaction mixture was applied to Supelclean Envi-Carb (Supelco, Bellefonte, PA, USA), and the tube was washed with H_2O to remove salts. Borohydride-reduced oligosaccharides were eluted with 30% acetonitrile containing 5 mM ammonium acetate. Oligosaccharides from erythropoietin were prepared by the method described in our previous report [7].

Exoglycosidase digestion of borohydrade-reduced oligosaccharides from HGF

Borohydride-reduced oligosaccharides prepared from 12.5 μg of HGF were incubated with 0.5 units of α-galactosidase in 100 mM sodium citrate/phosphate, pH 6.0, at 37 °C for 18 h. The reaction mixture was applied to Supelclean Envi-Carb, and the tube was washed with H_2O to remove salts. Borohydride-reduced oligosaccharides were eluted with 30% acetonitrile containing 5 mM ammonium acetate.

CapLC/MS

Capillary LC/MS, in positive-ionization, full-scan operation (*m/z* 800–2000), was carried out on a Magic 2002 system (Michrom BioResources, Inc., Auburn, CA, USA) connected to a TSQ 7000 triple-stage-quadruple mass spectrometer (ThermoFinnigan, San Jose, CA, USA) equipped with a nanoelectrospray ion source (AMR, Inc., Tokyo, Japan). The GCC used was a Hypercarb 5μ (0.2 × 150 mm; ThermoFinnigan). The eluents were 5 mM ammonium acetate, pH 9.6, containing 2% acetonitrile (pump A), and 5 mM ammonium acetate, pH 9.6, containing 80% acetonitrile (pump B). The borohydride-reduced oligosaccharides were eluted at a flow rate of 2 μl/min with a gradient of 18–38% for pump B in 40 min. The ESI voltage was set at 2000 V using a metal needle, and the capillary temperature was 175 °C. The electron multiplier was set at 1200 V. Collision-induced dissociation (CID) MS/MS spectra were obtained using argon as the collision gas at a pressure of 2.0 mTorr. The collision energy was adjusted to −25 eV. The scan rate was 3 s/scan.

Results

Sugar mapping of a glycoprotein by CapLC/MS

We tested the abilities of LC/MS with a capillary column (0.2 mm i.d.) and a nanoelectrospray ion source to separate and detect oligosaccharides using EPO. N-linked oligosaccharides in EPO are reported to be sialylated fucosyl bi-, tri, and tetraantennary complex-type [15–19]. Oligosaccharides were released from EPO by PNGase F and reduced to alditols with $NaBH_4$ to avoid the separation of anomers. The borohydride-reduced oligosaccharides were subjected to CapLC/MS

using ammonium acetate containing acetonitrile as a mobile phase. As shown in Fig. 1A, LC/MS with the capillary column successfully provided information on the glycosylation of a subnanogram quantity of EPO. Previously EPO at 20 and 2 μg was needed for the mass spectrometric sugar mapping using LC/MS with a semimicro column (2.1 mm i.d.) and a microbore column (1.0 mm i.d.), respectively (Fig. 1B). N-linked oligosaccharides from 50 ng of EPO were present in sufficient quantity to provide the sugar map using CapLC/MS. Most of the oligosaccharides detected in EPO by our previous method could be analyzed using a nanogram level of EPO by the present method (Figs. 1C–1N).

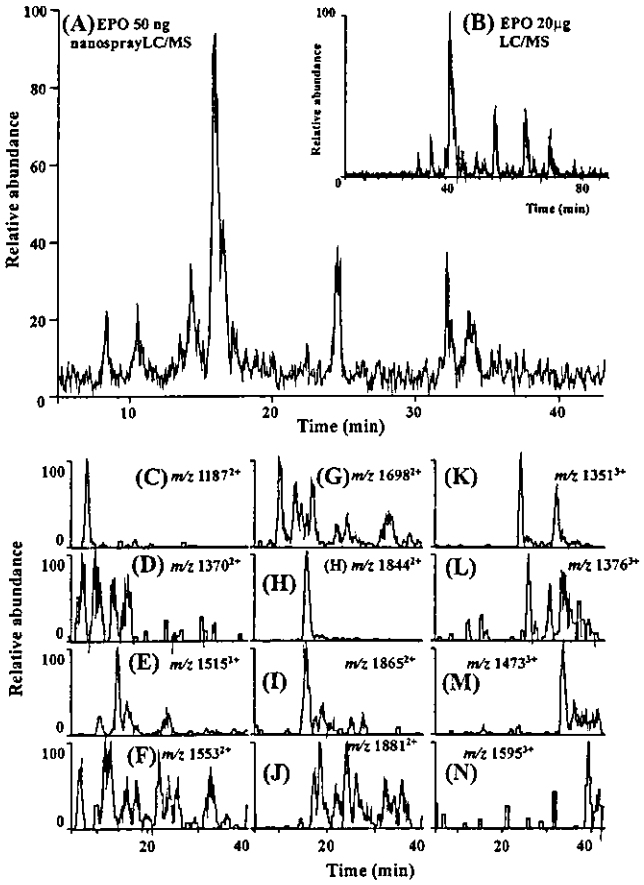

Fig. 1. Full-scan mass chromatography of borohydride-reduced oligosaccharides from EPO (50 ng) using LC/MS with a capillary column (0.2 mm i.d.) (A) and those from EPO (20 μg) using LC/MS with a semimicro column (2.1 mm i.d.) (B). Extracted mass chromatogram of borohydride-reduced oligosaccharides from EPO (50 ng) using CapLC/MS. (C) FucBi-$NeuAc_2^{2+}$ (*m/z* 1187), (D) FucBi-$Lac_1NeuAc_2^{2+}$/FucTri-$NeuAc_2^{2+}$ (*m/z* 1370), (E) FucTri-$NeuAc_3^{2+}$ (*m/z* 1515), (F) FucBi-$Lac_2NeuAc_2^{2+}$/FucTri-$Lac_1NeuAc_2^{2+}$/FucTetra-$NeuAc_2^{2+}$ (*m/z* 1553), (G) FucTri-$Lac_1NeuAc_3^{2+}$/FucTetra-$NeuAc_3^{2+}$ (*m/z* 1698), (H) FucTetra-$NeuAc_4^{2+}$ (*m/z* 1844), (I) FucTetra-$NeuAc_4Ac_1^{2+}$ (*m/z* 1865), (J) FucTri-$Lac_2NeuAc_3^{2+}$/FucTetra-$Lac_1NeuAc_3^{2+}$ (*m/z* 1881), (K) FucTetra-$Lac_1NeuAc_4^{3+}$ (*m/z* 1351), (L) FucTetra-$Lac_2NeuAc_3^{3+}$ (*m/z* 1376), (M) FucTetra-$Lac_2NeuAc_4^{3+}$ (*m/z* 1473), (N) FucTetra-$Lac_3NeuAc_4^{3+}$ (*m/z* 1595).

Sugar mapping of HGF by CapLC/MS

We examined the utility of the sugar mapping by CapLC/MS in the structural analysis of a low-abundance glycoprotein by using of HGF produced in NS0 cells, whose carbohydrate structures have not been reported. Fig. 2A shows the mass spectrometric sugar map of borohydride-reduced oligosaccharides from 200 ng of HGF. Two abundant peaks (peaks 5 and 9) were detected together with some low-abundance peaks. The *m/z* value at 1467 (peak 5) corresponds to the $[M + 2H]^{2+}$ ion of $[dHex]_1[Hex]_7[HexNAc]_5[NeuGc]_2$, suggesting a fucosyl triantennary complex-type bearing an additional Hex and two *N*-glycolylneuraminic acids (NeuGc) (FucTri – Hex_1NeuGc_2) (Fig. 3A, Table 1). The observed *m/z* value of peak 9 (*m/z* 1394^{2+}) was consistent with the theoretical *m/z* value of $[dHex]_1[Hex]_8[HexNAc]_5[NeuGc]_1$, fucosyl triantennary complex-type with two additional Hex and one NeuGc (FucTri – Hex_2NeuGc_1) (Fig. 3B, Table 1). Likewise, peaks 1–4, 6–8, and 10 and 11 could be deduced as fucosyl bi-, tri-, and tetraantennary bearing 0–3 Hex and 0–3 NeuGc (Table 1). There were no peaks suggesting the attachments of high-mannose-type, hybrid-type, or complex-type containing NeuAc. The sugar map suggests that the majority of N-linked oligosaccharides in

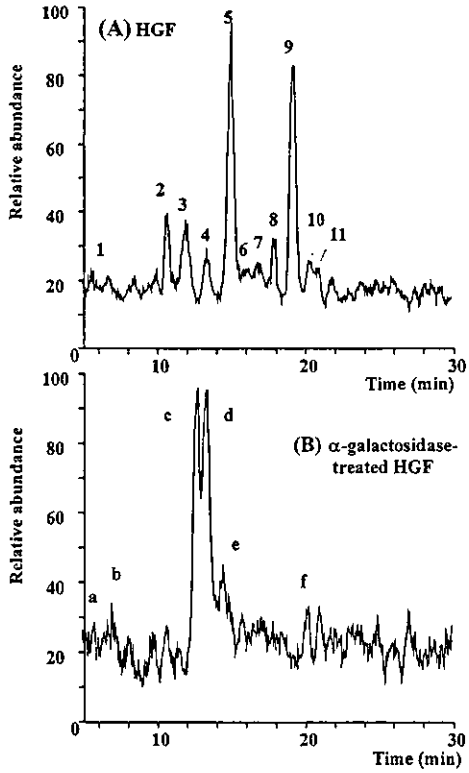

Fig. 2. Full-scan mass chromatography of borohydride-reduced oligosaccharides from HGF (200 ng) using CapLC/MS (A). Full-scan mass chromatography of α-galactosidase-treated borohydride-reduced oligosaccharides from HGF (200 ng) (B).

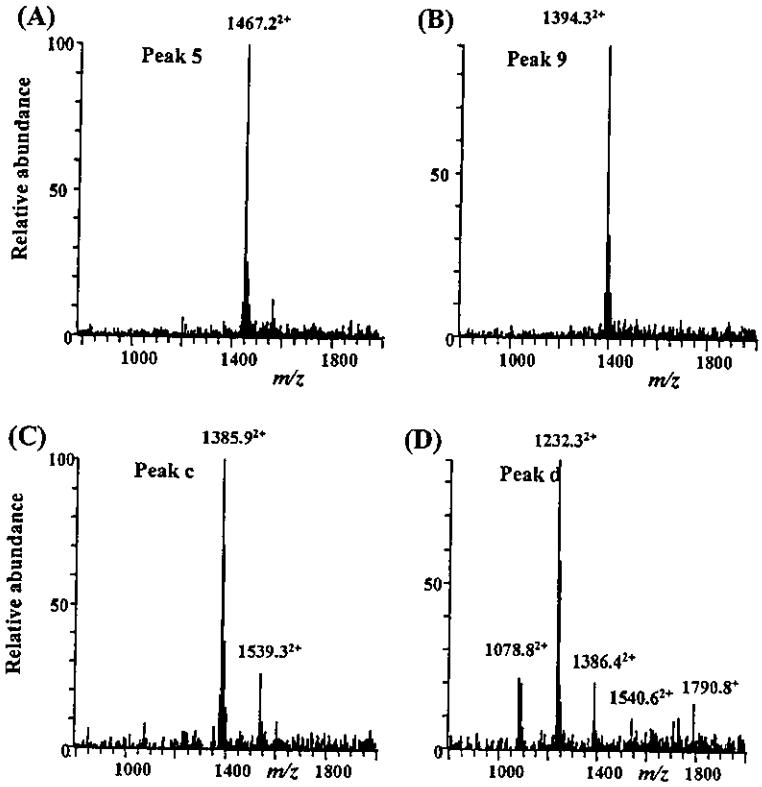

Fig. 3. Mass spectra of peak 5 (A), peak 9 (B), peak c (C), and peak d (D) in Fig. 2.

Table 1
Carbohydrate compositions and theoretical and calculated masses of peaks in Fig. 2A

Peak	Carbohydrate composition	Deduced carbohydrate structure	Theoretical mass[a]	Calculated mass	Charge state	Observed *m/z*
1	$[dHex]_1[Hex]_5[HexNAc]_4[NeuGc]_2$	FucBi-$NeuGc_2$[b]	2402.8	2403.6	2+	1202.8
2	$[dHex]_1[Hex]_6[HexNAc]_4[NeuGc]_1$	FucBi-Gal_1NeuGc_1	2257.8	2258.9	2+	1130.4
3	$[dHex]_1[Hex]_6[HexNAc]_5[NeuGc]_2$	FucTri-$NeuGc_2$[c]	2768.0	2769.8	2+	1385.9
	$[dHex]_1[Hex]_6[HexNAc]_5[NeuGc]_3$	FucTri-$NeuGc_3$	3075.1	3077.8	2+	1539.9
4	$[dHex]_1[Hex]_6[HexNAc]_5[NeuGc]_1$	FucTri-$NeuGc_1$	2460.9	2461.6	2+	1231.8
	$[dHex]_1[Hex]_6[HexNAc]_5[NeuGc]_3$	FucTri-$NeuGc_3$	3075.1	3077.2	2+	1539.6
5	$[dHex]_1[Hex]_7[HexNAc]_5[NeuGc]_2$	FucTri-Gal_1NeuGc_2	2930.0	2932.4	2+	1467.2
6	$[dHex]_1[Hex]_7[HexNAc]_4$	FucBi-Gal_2	2112.8	2114.6	2+	1058.3
	$[dHex]_1[Hex]_7[HexNAc]_5[NeuGc]_2$	FucTri-Gal_1NeuGc_2	2930.0	2932.0	2+	1467.0
7	$[dHex]_1[Hex]_7[HexNAc]_5[NeuGc]_1$	FucTri-Gal_1NeuGc_1	2622.9	2624.4	2+	1313.2
	$[dHex]_1[Hex]_7[HexNAc]_5[NeuGc]_2$	FucTri-Gal_1NeuGc_2	2930.0	2931.6	2+	1466.8
8	$[dHex]_1[Hex]_7[HexNAc]_5[NeuGc]_2$	FucTri-Gal_1NeuGc_2	2930.0	2931.6	2+	1466.8
9	$[dHex]_1[Hex]_8[HexNAc]_5[NeuGc]_1$	FucTri-Gal_2NeuGc_1	2785.0	2786.6	2+	1394.3
10	$[dHex]_1[Hex]_7[HexNAc]_6[NeuGc]_1$	FucTetra-$NeuGc_1$[d]	2826.0	2827.8	2+	1414.9
11	$[dHex]_1[Hex]_9[HexNAc]_5$	FucTri-Gal_3	2640.0	2641.0	2+	1321.5
	$[dHex]_1[Hex]_8[HexNAc]_5[NeuGc]_1$	FucTri-Gal_2NeuGc_1	2785.0	2787.4	2+	1394.7

[a] Monoisotopic mass value.

b
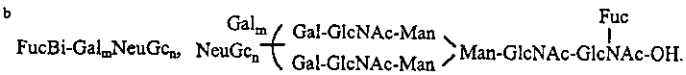

c
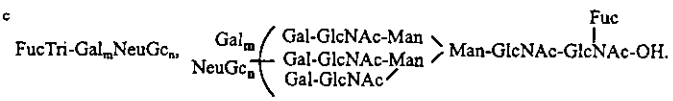

d
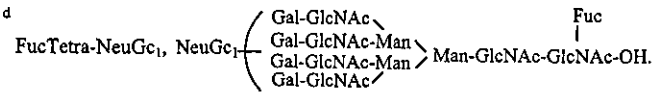

NS0 cell-derived HGF are triantennary complex-type containing NeuGc and additional Hex.

Sugar mapping of exoglycosidase-digested oligosaccharides

Exoglycosidase digestion followed by mass spectrometric sugar mapping was performed to determine the Hex and its linkage. Treatment with α-galactosidase, which cleaves Galα1–3,4,6Gal/Glc, resulted in new peaks, such as peaks c and d, in place of some peaks that disappeared (typically peaks 5 and 9) (Fig. 2). The dominant ion at *m/z* 1386^{2+} in peak c can be deduced as fucosyl triantennary bearing two NeuGc, which is possibly produced from FucTri-Gal_1NeuGc_2 (peak 5) by losing one Gal (Fig. 3C, Table 2). The intense ion in peak d (*m/z* 1232^{2+}) was suggested to be triantennary bearing one NeuGc, which is formed from FucTri-Gal_2NeuGc_1 (peak 9) by losing two Gal (Fig. 3D, Table 2). Likewise, other ions at *m/z* 1050^{2+}, 1079^{2+}, and 1203^{2+} can be assigned to bi- and triantennary without additional Hex (Table 2). These results clearly indicate α-linked galactosylation on nonreducing ends of oligosaccharides in HGF.

CapLC/MS/MS

CapLC/MS/MS was performed for the analysis of structural detail of FucTri-Gal_1NeuGc_2 (peak 5) and FucTri-Gal_2NeuGc_1 (peak 9). Fig. 4 shows the product

Table 2
Carbohydrate compositions and theoretical and calculated masses of peaks in Fig. 2B

Peak	Carbohydrate composition	Deduced carbohydrate structure	Theoretical mass[a]	Calculated mass	Charge state	Observed *m/z*
a	$[dHex]_1[Hex]_5[HexNAc]_4[NeuGc]_2$	FucBi-$NeuGc_2$	2402.8	2405.4	2+	1203.7
b	$[dHex]_1[Hex]_5[HexNAc]_4[NeuGc]_1$	FucBi-$NeuGc_1$	2095.8	2098.2	2+	1050.1
c	$[dHex]_1[Hex]_6[HexNAc]_5[NeuGc]_2$	FucTri-$NeuGc_2$	2768.0	2769.8	2+	1385.9
	$[dHex]_1[Hex]_6[HexNAc]_5[NeuGc]_3$	FucTri-$NeuGc_3$	3075.1	3076.6	2+	1539.3
d	$[dHex]_1[Hex]_5[HexNAc]_4$	FucBi	1788.7	1789.8	1+	1790.8
	$[dHex]_1[Hex]_6[HexNAc]_5$	FucTri	2153.8	2155.6	2+	1078.8
	$[dHex]_1[Hex]_6[HexNAc]_5[NeuGc]_1$	FucTri-$NeuGc_1$	2460.9	2462.6	2+	1232.3
	$[dHex]_1[Hex]_6[HexNAc]_5[NeuGc]_2$	FucTri-$NeuGc_2$	2768.0	2770.8	2+	1386.4
	$[dHex]_1[Hex]_6[HexNAc]_5[NeuGc]_3$	FucTri-$NeuGc_3$	3075.1	3079.2	2+	1540.6
e	$[dHex]_1[Hex]_6[HexNAc]_5[NeuGc]_3$	FucTri-$NeuGc_3$	3075.1	3077.6	2+	1539.8
f	$[dHex]_1[Hex]_7[HexNAc]_6[NeuGc]_1$	FucTetra-$NeuGc_1$	2826.0	2825.2	2+	1413.6

[a] Monoisotopic mass value.

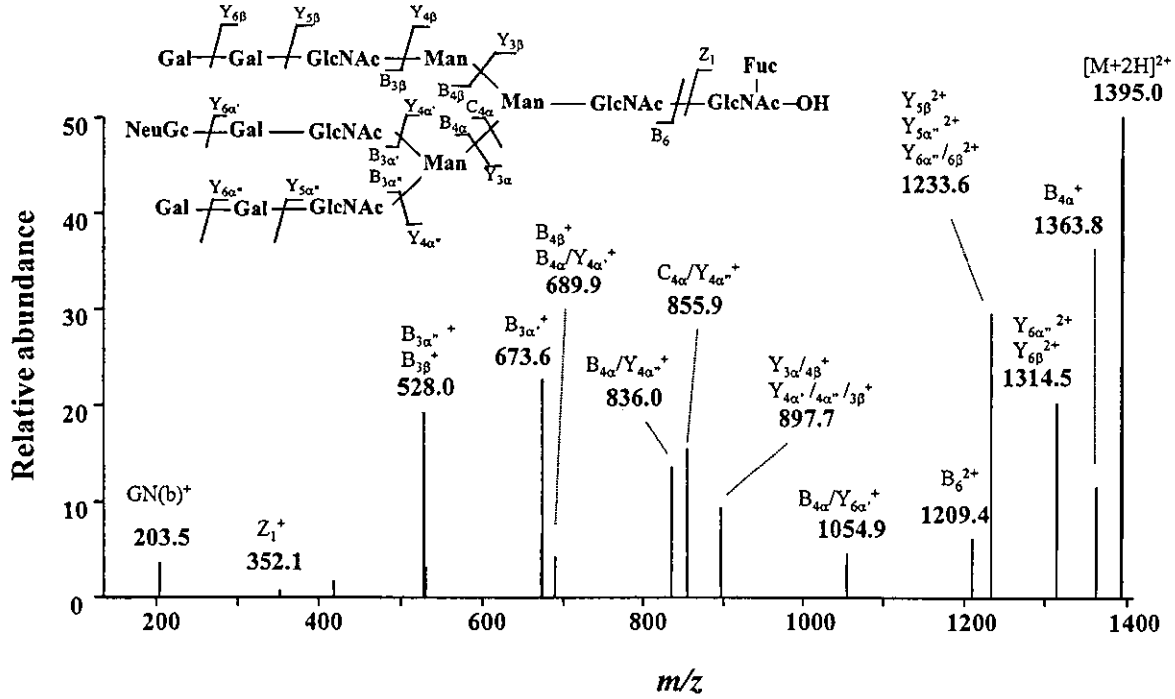

Fig. 4. MS/MS spectrum of the FucTri-$Gal_2NeuGc_1^{2+}$ at *m/z* 1395.

ion mass spectrum of FucTri-Gal_2NeuGc_1 at *m/z* 1395^{2+} (peak 9). We can find the set of b-ion series [20], *m/z* 528 $[Hex]_2[HexNAc]^+$, 673 $[NeuGc][Hex][HexNAc]^+$, 690 $[Hex]_3[HexNAc]^+$, 836 $[NeuGc][Hex]_2[HexNAc]^+$, 1362 $[NeuGc][Hex]_4[HexNAc]_2^+$, and 1209 $[NeuGc][Hex]_8[HexNAc]_4^{2+}$. These fragment ions suggest the monosaccharide sequence of FucTri-Gal_2NeuGc_1 shown in Fig. 4.

Four isomers, peaks A–D, were detected by CID-MS/MS of FucTri-Gal_1NeuGc_2 at *m/z* 1467^{2+} (Fig. 5A). Fragment ion at *m/z* 1362 $[NeuGc][Hex]_4[HexNAc]_2^+$ was detected together with other b-type fragment ions in Figs. 5B (peak A) and 5C (peak C), while the ion at *m/z*1507 $[NeuGc]_2[Hex]_3[HexNAc]_2^+$ is shown in Figs. 5D (peak B) and 5E (peak D). The fragment ion at *m/z* 1362^+ (peaks A and C) suggests the linkages of one NeuGc to both nonreducing ends of Manα1–3 and Manα1–6 branches, and that at *m/z* 1507^+ (peaks B and D) suggests the linkage of two NeuGc to either the Manα1–3 or the Manα1–6 branch. CapLC/MS/MS proved to be useful for the sequential analysis of N-linked oligosaccharides and the distinction between isomers.

Discussion

We have studied rapid and simple mass spectrometric sugar mapping [6,7] and applied it to the structural analysis [8], quality control, and comparability assessment of therapeutic biotechnological/biological products [9]. There is also a need to analyze glycosylation in various aspects, including proteomics study, diagnosis, and clinical stages, for which the amount of sample available is limited. In this study we successfully extended the mass spectrometric sugar mapping of a small amount of glycoprotein by the employment of CapLC/MS. Oligosaccharides, including isomers, could be separated by capillary GCC, and their structures were deduced on the basis of molecular masses and their retention times.

Electrophoresis, especially two-dimensional electrophoresis, has been widely used for the separation of protein mixtures. Protein spots are excised and digested *in situ* with trypsin. Protein identification at the femtomole level is achieved by mass spectrometry of proteolytic peptides and databases (peptide mapping or peptide mass fingerprinting) [21,22]. Glycopeptides are usually identified by precursor ion scanning, by which ions at *m/z* 163 $[Hex]^+$ and 204 $[HexNAc]^+$ produced by CID from glycopeptides are monitored [23], and carbohydrate structures are deduced from molecular mass of glycopeptides [24,25]. However, large glycopeptides and highly heterogeneous glycopeptides are hardly detected by MS analysis, due to their poor ionization. Moreover, mass spectrometric peptide mapping cannot distinguish the monosaccharide composition, sequence, branching, and linkage. Recently, analyses of derived oligosaccharides from in-gel glycoproteins by matrix-assisted laser desorption/ionization mass spectrometry were reported [26–28]. Sugar mapping of enzymatically released N-linked oligosaccharides from a gel is more useful for the understanding of carbohydrate structure and function. The success of the sugar mapping with CapLC/MS allows for the detailed characterization of gel-separated glycoprotein rapidly and automatically. We have actually succeeded in applying this method to the structural analysis of oligosaccharides from a gel-separated glycoprotein.

We also demonstrated the utility of CapLC/MS/MS and exoglycosidase digestion followed by CapLC/MS in the structural analyses of oligosaccharides. HGF is a multifunctional cytokine that is expected to be a new therapeutic glycoprotein, including in cell therapy and gene therapy approaches. Although the characterization of HGF is important, carbohydrate structures of HGF were studied only in Chinese hamster ovary cell derivatives due to its limited availability [29]. They were deduced to be fucosylated bi-, tri-, and tetraantennary bearing NeuAc by two-dimensional sugar mapping. NS0 cells are currently the favored host cell type for the production of therapeutic recombinant proteins. In this study, N-linked oligosaccharides in NS0 cell-derived HGF were easily characterized as the complex-type bi-, tri-, and tetraantennary with NeuGc and additional Hex by CapLC/MS. CapLC/MS/MS provides b-ion series, which are informative with regard to the monosaccharide sequence. Exoglycosidase digestion followed by CapLC/MS elucidated the linkage of the additional Hex. Using CapLC/MS/MS and exoglycosidase digestion, the majority of N-linked oligosaccharides in HGF were deduced to be triantennary terminated with α-linked galactose residues and NeuGc residues. There are some reports on α1,3-linked galactosylation in NS0-derived glycoproteins [30,31]. Nonreducing ends of HGF may be also terminated with Gal by α1,3-linkage. CapLC/MS/MS and exoglycosidase followed by CapLC/MS were able to elucidate the detailed carbohydrate structure of HGF through yielding the information of monosaccharide sequence, and linkages.

Some sugar residues are recognized as antigens by natural human antibodies. Anti-α-galactosyl antibodies are known in human serum [32]. Rapid rejection due to the terminal α-Gal residue is reported after transplantation of foreign species. NeuGc is also known to be an antigenic molecule [33,34]. For clinical prevention, potentially immunogenic glycoforms should be minimized in therapeutic biotechnological/biological products. CapLC/MS proved to be useful for the monitoring of glycosylation pattern, including immunogenic carbohydrate units, and thus could become a powerful tool

in the pharmaceutical manufacturing process. In addition, alterations in carbohydrate structure are known to be linked to many diseases, such as rheumatoid arthritis [35]. Monitoring of glycosylation is beneficial in the diagnosis of disease. Our method can be also applicable for the diagnosis of disease.

References

[1] A. Varki, Biological roles of oligosaccharides: all of the theories are correct, Glycobiology 3 (1993) 97–130.

[2] G. Durand, N. Seta, Protein glycosylation and diseases: blood and urinary oligosaccharides as markers for diagnosis and therapeutic monitoring, Clin. Chem. 46 (2000) 795–805.

[3] T.S. Mattu, R.J. Pleass, A.C. Willis, M. Kilian, M.R. Wormald, A.C. Lellouch, P.M. Rudd, J.M. Woof, R.A. Dwek, The glycosylation and structure of human serum IgA1, Fab, and Fc regions and the role of N-glycosylation on Fc alpha receptor interactions, J. Biol. Chem. 273 (1998) 2260–2272.

[4] N. Takahashi, H. Nakagawa, K. Fujikawa, Y. Kawamura, N. Tomiya, Three-dimensional elution mapping of pyridylaminated N-linked neutral and sialyl oligosaccharides, Anal. Biochem. 226 (1995) 139–146.

[5] N. Tomiya, J. Awaya, M. Kurono, S. Endo, Y. Arata, N. Takahashi, Analyses of N-linked oligosaccharides using a two-dimensional mapping technique, Anal. Biochem. 171 (1988) 73–90.

[6] N. Kawasaki, M. Ohta, S. Hyuga, O. Hashimoto, T. Hayakawa, Analysis of carbohydrate heterogeneity in a glycoprotein using liquid chromatography/mass spectrometry and liquid chromatography with tandem mass spectrometry, Anal. Biochem. 269 (1999) 297–303.

[7] N. Kawasaki, M. Ohta, S. Hyuga, M. Hyuga, T. Hayakawa, Application of liquid chromatography/mass spectrometry and liquid chromatography with tandem mass spectrometry to the analysis of the site-specific carbohydrate heterogeneity in erythropoietin, Anal. Biochem. 285 (2000) 82–91.

[8] N. Kawasaki, Y. Haishima, M. Ohta, S. Itoh, M. Hyuga, S. Hyuga, T. Hayakawa, Structural analysis of sulfated N-linked oligosaccharides in erythropoietin, Glycobiology 11 (2001) 1043–1049.

[9] N. Kawasaki, M. Ohta, S. Itoh, M. Hyuga, S. Hyuga, T. Hayakawa, Usefulness of sugar mapping by liquid chromatography/mass spectrometry in comparability assessments of glycoprotein product, Biologicals 30 (2002) 113–123.

[10] S. Itoh, N. Kawasaki, M. Ohta, M. Hyuga, S. Hyuga, T. Hayakawa, Simultaneous microanalysis of N-linked oligosaccharides in a glycoprotein using microbore graphitized carbon column liquid chromatography/mass spectrometry, J. Chromatogr. A 968 (2002) 89–100.

[11] K.A. Thomsson, N.G. Karlsson, G.C. Hansson, Liquid chromatography–electrospray mass spectrometry as a tool for the analysis of sulfated oligosaccharides from mucin glycoproteins, J. Chromatogr. A 854 (1999) 131–139.

[12] K.A. Thomsson, H. Karlsson, G.C. Hansson, Sequencing of sulfated oligosaccharides from mucins by liquid chromatography and electrospray ionization tandem mass spectrometry, Anal. Chem. 72 (2000) 4543–4549.

[13] J. Delaney, P. Vouros, Liquid chromatography ion trap mass spectrometric analysis of oligosaccharides using permethylated derivatives, Rapid Commun. Mass Spectrom. 15 (2001) 325–334.

[14] L. Royle, T.S. Mattu, E. Hart, J.I. Langridge, A.H. Merry, N. Murphy, D.J. Harvey, R.A. Dwek, P.M. Rudd, An analytical and structural database provides a strategy for sequencing *O*-glycans from microgram quantities of glycoproteins, Anal. Biochem. 304 (2002) 70–90.

[15] K.B. Linsley, S.Y. Chan, S. Chan, B.B. Reinhold, P.J. Lisi, V.N. Reinhold, Applications of electrospray mass spectrometry to erythropoietin N- and O-linked glycans, Anal. Biochem. 219 (1994) 207–217.

[16] H. Sasaki, B. Bothner, A. Dell, M. Fukuda, Carbohydrate structure of erythropoietin expressed in Chinese hamster ovary cells by a human erythropoietin cDNA, J. Biol. Chem. 262 (1987) 12059–12076.

[17] H. Sasaki, N. Ochi, A. Dell, M. Fukuda, Site-specific glycosylation of human recombinant erythropoietin: analysis of glycopeptides or peptides at each glycosylation site by fast atom bombardment mass spectrometry, Biochemistry 27 (1988) 8618–8626.

[18] M. Takeuchi, S. Takasaki, H. Miyazaki, T. Kato, S. Hoshi, N. Kochibe, A. Kobata, Comparative study of the asparagine-linked sugar chains of human erythropoietins purified from urine and the culture medium of recombinant Chinese hamster ovary cells, J. Biol. Chem. 263 (1988) 3657–3663.

[19] E. Tsuda, M. Goto, A. Murakami, K. Akai, M. Ueda, G. Kawanishi, N. Takahashi, R. Sasaki, H. Chiba, H. Ishihara, et al., Comparative structural study of N-linked oligosaccharides of urinary and recombinant erythropoietins, Biochemistry 27 (1988) 5646–5654.

[20] B. Domon, C.E. Costello, A systematic nomenclature for carbohydrate fragmentation in FAB-MS/MS spectra of glycoconjugates, Glycoconjugate J. 5 (1988) 394–409.

[21] C. Fenselau, MALDI MS and strategies for protein analysis, Anal. Chem. 69 (1997) 661A–665A.

[22] M.T. Davis, T.D. Lee, Rapid protein identification using a microscale electrospray LC/MS system on an ion trap mass spectrometer, J. Am. Soc. Mass Spectrom. 9 (1998) 194–201.

[23] M.J. Huddleston, M.F. Bean, S.A. Carr, Collisional fragmentation of glycopeptides by electrospray ionization LC/MS and LC/MS/MS: methods for selective detection of glycopeptides in protein digests, Anal. Chem. 65 (1993) 877–884.

[24] K. Hirayama, R. Yuji, N. Yamada, K. Kato, Y. Arata, I. Shimada, Complete and rapid peptide and glycopeptide mapping of mouse monoclonal antibody by LC/MS/MS using ion trap mass spectrometry, Anal. Chem. 70 (1998) 2718–2725.

[25] T. Kurahashi, A. Miyazaki, Y. Murakami, S. Suwan, T. Franz, M. Isobe, N. Tani, H. Kai, Determination of a sugar chain and its linkage site on a glycoprotein TIME-EA4 from silkworm diapause eggs by means of LC-ESI-Q-TOF-MS and MS/MS, Bioorg. Med. Chem. 10 (2002) 1703–1710.

[26] J. Charlwood, J.M. Skehel, P. Camilleri, Analysis of N-linked oligosaccharides released from glycoproteins separated by two-dimensional gel electrophoresis, Anal. Biochem. 284 (2000) 49–59.

[27] B. Kuster, S.F. Wheeler, A.P. Hunter, R.A. Dwek, D.J. Harvey, Sequencing of N-linked oligosaccharides directly from protein gels: in-gel deglycosylation followed by matrix-assisted laser desorption/ionization mass spectrometry and normal-phase high-performance liquid chromatography, Anal. Biochem. 250 (1997) 82–101.

[28] B. Kuster, T.N. Krogh, E. Mortz, D.J. Harvey, Glycosylation analysis of gel-separated proteins, Proteomics 1 (2001) 350–361.

[29] H. Hara, Y. Nakae, T. Sogabe, I. Ihara, S. Ueno, H. Sakai, H. Inoue, S. Shimizu, T. Nakamura, N. Shimizu, Structural study of the N-linked oligosaccharides of hepatocyte growth factor by two-dimensional sugar mapping, J. Biochem. (Tokyo) 114 (1993) 76–82.

[30] D.M. Sheeley, B.M. Merrill, L.C. Taylor, Characterization of monoclonal antibody glycosylation: comparison of expression systems and identification of terminal α-linked galactose, Anal. Biochem. 247 (1997) 102–110.

[31] K.N. Baker, M.H. Rendall, A.E. Hills, M. Hoare, R.B. Freedman, D.C. James, Metabolic control of recombinant protein *N*-

glycan processing in NS0 and CHO cells, Biotechnol. Bioeng. 73 (2001) 188–202.

[32] W. Parker, S.S. Lin, P.B. Yu, A. Sood, Y.C. Nakamura, A. Song, M.L. Everett, J.L. Platt, Naturally occurring anti-alpha-galactosyl antibodies: relationship to xenoreactive anti-alpha-galactosyl antibodies, Glycobiology 9 (1999) 865–873.

[33] T. Higashihara, T. Takeshima, M. Anzai, M. Tomioka, K. Matsumoto, K. Nishida, Y. Kitamura, K. Okinaga, M. Naiki, Survey of Hanganutziu and Deicher antibodies in operated patients, Int. Arch. Allergy Appl. Immunol. 95 (1991) 231–235.

[34] J.M. Merrick, K. Zadarlik, F. Milgrom, Characterization of the Hanganutziu–Deicher (serum-sickness) antigen as gangliosides containing *N*-glycolylneuraminic acid, Int. Arch. Allergy Appl. Immunol. 57 (1978) 477–480.

[35] R.B. Parekh, R.A. Dwek, B.J. Sutton, D.L. Fernandes, A. Leung, D. Stanworth, T.W. Rademacher, T. Mizuochi, T. Taniguchi, K. Matsuta, F. Takeuchi, Y. Nagano, T. Miyamoto, A. Kobata, Association of rheumatoid arthritis and primary osteoarthritis with changes in the glycosylation pattern of total serum IgG, Nature 316 (1985) 452–457.

再生医療の社会的側面

細胞・組織加工医薬品・医療機器の品質管理

早川 堯夫 国立医薬品食品衛生研究所副所長

永田 龍二 国立医薬品食品衛生研究所
遺伝子細胞医薬部主任研究官

CLINICAL NEUROSCIENCE 別冊

Vol. 21 No. 10　2003年10月1日発行

中外医学社

細胞・組織加工医薬品・医療機器の品質管理

早川 堯夫　永田 龍二

「細胞・組織加工医薬品・医療機器」は，疾患の治療や組織の修復または再建を目的として，ヒトまたは動物の細胞・組織を加工した医薬品または医療機器(以下「医薬品等」)と定義される．ここでいう「加工」の分類および具体例を表1に示す．組織の分離や細切，細胞の分離，特定細胞の分離，抗生物質による処理，洗浄，ガンマ線等による滅菌，冷凍，解凍のような操作は「加工」とはみなさない．

本邦では，医薬品等の製造・輸入承認申請のための臨床試験(2002年7月の薬事法改正に伴い新たに可能となった医師主導型の臨床試験も含める．以下「治験」)を実施する際，事前に厚生労働大臣に治験計画の届け出を行う必要があるが，細胞・組織加工医薬品等の場合には，さらに治験計画届の提出前に当該医薬品等の安全性や品質の確認を厚生労働大臣に求めなければならない[1]．それに関連して，厚生労働省から「細胞・組織利用医薬品等の取扱い及び使用に関する基本的考え方」[2)-1]および「ヒト由来細胞・組織加工医薬品等の品質及び安全性の確保に関する指針」[2)-2]が公表されている．本邦では医薬品・医療機器として承認された細胞・組織加工製品はまだ存在しないが(2003年5月現在)，ヒト由来の培養皮膚や樹状細胞等の治験あるいは各医療機関における自主的な臨床研究(医師主導の臨床試験以外のもの)は既に実施されており，積極的に開発が進められている[3]．治験，臨床研究の別を問わず，細胞・組織加工医薬品等の品質および安全性の確保のためには，上記「基本的考え方」[2)-1]を踏まえながら「指針」[2)-2]で具体的にあげられている事項について十分理解・考慮する必要がある[4]．

なお，詳細は本誌他項に譲るが，細胞・組織加工医薬品等の製造中に遺伝子操作を行う場合は，厚生労働省や文部科学省の指針[5,6]の適用対象にもなる．動物由来の細胞・組織を用いる際には，厚生労働省から公表されている指針[7]も参考になるであろう．

はやかわ たかお　国立医薬品食品衛生研究所副所長
ながた りゅうじ　国立医薬品食品衛生研究所/遺伝子細胞医薬部主任研究官

1．細胞・組織の人為的な増殖
　例）採取した細胞・組織を体外で培養・増殖させた後，それを患者に適用する場合．
2．細胞・組織の活性化等を目的とした処理
　① 薬剤処理
　　例）採取した未分化の細胞の体外での培養に際し分化誘導物質を添加して目的とするステージの細胞に分化させた後，それを患者に適用する場合．
　② 生物学的特性の改変
　　例）採取した細胞を体外で培養する際にサイトカインや抗原で人為的に刺激することによって細胞の生物学的特性を目的のものに改変した後，それを患者に適用する場合．
　③ 細胞・組織の遺伝子工学的改変
　　例）採取した細胞・組織に体外で遺伝子導入を行った後，それを患者に適用する場合(このような医療行為は「遺伝子治療」の範疇にも属することに注意)．
3．非細胞・組織とのハイブリッド化
　例）採取した細胞・組織の体外での培養に際し特定の効果を期待して人為的に添加された非細胞・組織成分が，最終製品においても含有されている場合．一例としては，採取した細胞を培養用マトリクス上で培養し，それにより得られた増殖細胞の貼りついたマトリクス全体を患者に適用する場合．
4．カプセル化
　例）細胞・組織加工医薬品・医療機器の本質である細胞・組織が適用患者等に直接的に接触しないよう，非細胞・組織成分を用いて当該細胞・組織が隔離されるような剤型として最終製品が製造されている場合．一例としては，目的のペプチド・たん白を産生・分泌する細胞を患者に適用する際に，そのまま適用したのでは免疫反応の惹起や人獣共通感染症病原体の混入が懸念されるため，目的のペプチド・たん白が透過するような材質のカプセルで動物細胞をくるみ，それを患者に適用する場合．
5．その他

注）上記の区分は各々独立したものではなく，品目ごとに複数の区分に該当する場合もある．

0289-0585/03/¥500/論文/JCLS

1．本文書の目的，基本原則，定義

○細胞・組織利用医薬品等＝ヒトまたは動物の細胞・組織から構成された生物由来医薬品または生物由来医療機器，自己の細胞・組織を原材料とするものも含む．但し，血液製剤は含まない．

○本文書は細胞・組織利用医薬品等の承認後のみならず治験時にも適用．

○細胞・組織利用医薬品等は，細胞・組織に由来する感染症の伝播等の危険性を完全には排除し得ないおそれがあることから，他の治療薬や治療法と比較して有用性が同程度以上と判断されるときにのみ使用すべき．

2．細胞・組織採取について

○適切な衛生管理，知識・技術をもった人員の確保

○倫理委員会での事前調査・審議

○ドナーからのインフォームドコンセントの取得，無対価での提供

○ドナーおよびドナー動物の選択基準および適格性

・ドナーの適格性：免疫適合性等を考慮．問診および適切な検査による HBV，HCV，HIV，HTLV およびヒトパルボウイルス B19 感染の否定．必要に応じて検査による CMV および EB ウイルス感染の否定．梅毒，クラミジア，淋菌・結核菌等の細菌感染症，敗血症(疑い)，悪性腫瘍，重篤な代謝・内分泌疾患，膠原病，血液疾患，肝疾患並びに痴呆症[伝達性海綿状脳症(疑い)]に関して，既往歴や問診等による診断および輸血や移植医療の経験の有無等から適格性を判断．

・ウインドウピリオド(病原体またはそれに対する抗体が検出できない感染初期の時期)の存在を考慮して可能な限り再検査を実施．

・患者自己由来の細胞・組織を用いる場合は必ずしもドナースクリーニングを必要としない．

○感染性物質による汚染を防ぐために必要な措置・検査の実施，○記録

3．製造段階における安全性確保対策

○独立した作業区域の設置．複数のドナーからの細胞・組織を同一室内で同時期に取り扱うことや，交叉汚染を引き起こす可能性のある保管方法の禁止

○標準操作手順書の作成および遵守．製造工程に関する記録

○採取した細胞・組織および試薬等の受入れ試験・検査．製品の試験・検査．感染性物質による汚染の危険性の排除

○最新技術の反映

4．職員および組織並びに管理体制(職員の教育訓練，健康管理)等

5．使用段階における安全性確保対策

○ドナーや最終製品の試験・検査結果の医療機関に対する提供

○患者からのインフォームドコンセントの取得

○患者等の試料の保存．患者等に関する情報の把握

・適用前後の患者の感染症に関する記録および血清等の試料並びに実際に適用した製品の保存．

6．個人情報の保護，7．見直し

1．本文書の目的，定義

2．利用目的，製造方法および安定性

○原材料となる細胞・組織および製造方法について

・原材料となる細胞・組織の特性と適格性の確認．採取した細胞・組織の一部保管．感染性物質の不活化/除去．加工した細胞の特性解析．

・培地や細胞の処理に用いる試薬等の全成分について，感染性物質の否定も含めて適格性を明らかにし，必要な品質規格を設定．培養・加工時の血清の使用は可能な限り避ける．避けられない場合，血清由来感染性物質の混入・伝播の防止および使用血清の一部を保管．

・細胞に遺伝子工学的改変を加える場合における詳細は文献 6 参照．

○細胞・組織以外の原材料について

・最終製品の一部を構成する細胞・組織以外の原材料がある場合，当該原材料の品質および安全性並びに細胞に及ぼす影響を検討．当該原材料の特性に応じて文献 8 を参考に必要な規格を設定．

・細胞・組織と適用部位を隔離する目的で非細胞・組織成分を用いる場合，次の項目を参考に効果・安全性を確認．免疫隔離の程度，栄養成分および排泄・分泌物の拡散，細胞・組織由来の生理活性物質の膜透過キネティクスと薬理効果，患者由来の生理活性物質の細胞・組織への有害作用．

○細胞・組織の同一性および均一性の確認，品質管理，製品の安定性の確認

・次に示す一般的な品質管理試験項目を参考に必要な規格を設定．細胞の回収率・生存率，同一性の確認，細胞・組織由来の目的生理活性物質の量/力価，無菌性およびマイコプラズマ，エンドトキシン，製造工程由来不純物，細胞の純度，細胞・組織由来の目的外生理活性物質の種類および量/力価，力学的適合性，感染性物質．

3．非臨床安全性試験，効力/性能を裏付ける試験，体内動態

・特に次の項目について必要に応じて動物および *in vitro* での試験を実施し，安全性を確認．加工細胞の性質の変化，細胞・組織が産生する各種生理活性物質の定量および患者への影響，患者の正常細胞・組織に対する製品の影響，望ましくない免疫反応が生じる可能性．さらに，最終製品が大量に生産される場合には一般毒性試験．

4．臨床試験(外国における開発状況も含める)

○治験計画の概要

・製品適用後の有効性/安全性評価期間・項目は十分検討して決定．免疫学的事項も含める．

5．確認および報告